
Multi-dataset Pretraining: A Unified Model for Semantic Segmentation

Bowen Shi¹, Xiaopeng Zhang², Haohang Xu¹,
Wenrui Dai¹, Junni Zou¹, Hongkai Xiong¹, Qi Tian²

¹Shanghai Jiao Tong University ²Huawei Inc.

{sjtu_shibowen, xuhaohang, daiwenrui, zoujunni, xionghongkai}@sjtu.edu.cn
zxphistory@gmail.com tian.qi1@huawei.com

Abstract

Collecting annotated data for semantic segmentation is time-consuming and hard to scale up. In this paper, we *for the first time* propose a unified framework, termed as **Multi-Dataset Pretraining**, to take full advantage of the fragmented annotations of different datasets. The highlight is that the annotations from different domains can be efficiently reused and consistently boost performance for each specific domain. This is achieved by first pretraining the network via the proposed pixel-to-prototype contrastive loss over multiple datasets regardless of their taxonomy labels, and followed by fine-tuning the pretrained model over specific dataset as usual. In order to better model the relationship among images and classes from different datasets, we extend the pixel level embeddings via cross dataset mixing and propose a pixel-to-class sparse coding strategy that explicitly models the pixel-class similarity over the manifold embedding space. In this way, we are able to increase intra-class compactness and inter-class separability, as well as considering inter-class similarity across different datasets for better transferability. Experiments conducted on several benchmarks demonstrate its superior performance. Notably, MDP consistently outperforms the pretrained models over ImageNet by a considerable margin, while only using less than 10% samples for pretraining.

1 Introduction

As a basic computer vision task, semantic segmentation has experienced remarkable progress over the past decades, mainly benefiting from the growth of the available annotations. However, annotating images at pixel level granularity is time-consuming and difficult to scale up. In order to alleviate the dense annotation requirement, semantic segmentation is usually fine-tuned based on a pretrained model, *e.g.*, training on a large-scale ImageNet classification dataset [23]. While ImageNet pretraining can *de facto* lead to significant performance gains, it suffers from task gap that the pretraining is based on global classification while the downstream task is for local pixel level prediction. In this paper, we arise a critical issue, can we solve the task gap via making use of the available annotations off-the-shelf from diverse segmentation datasets for better performance?

Though promising it is, a major challenge of unifying multi-datasets for training is to tackle the label inconsistency, where taxonomy from different datasets differs, ranging from class definition and class granularity. For example, the classes 'wall-brick', 'wall-concrete' and 'wall-panel' in COCO-Stuff [2] are simply labeled as 'wall' in ADE20K [32], and as 'background' in Pascal VOC [9]. However, integrating different datasets into a common taxonomy is time-consuming and error-prone. In this paper, we propose a novel training framework that is able to directly unify different datasets for training regardless of its taxonomy labels. In Fig. 1, we illustrate several typical pretraining settings for semantic segmentation. The advantage of MDP is that we are able to conveniently combine

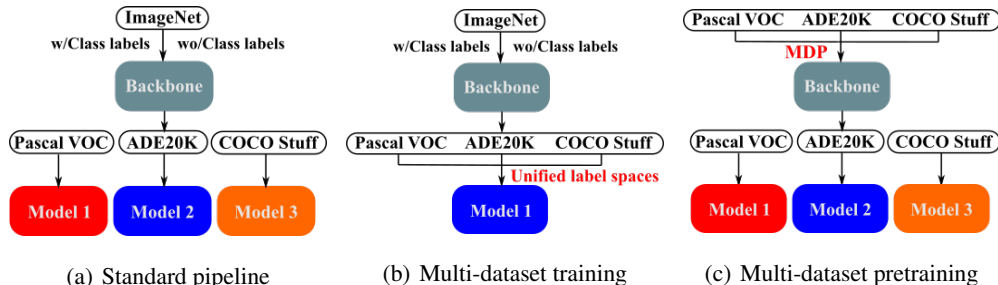


Figure 1: Typical settings for semantic segmentation. a) Most of the previous works follow the standard pipeline, which performs supervised or self-supervised pretraining on ImageNet, and then trains segmentation models on one specific dataset alone. b) Multi-dataset training means training a unified segmentation model using all annotated data, but needs manually unifying the label space of different datasets. c) Our work directly uses multiple datasets for pretraining, allowing the model to learn pixel level distinguishable features automatically.

multiple datasets for jointly training without any human intervention, and the pretrained model can be used as a backbone for downstream fine-tuning as usual.

Towards this goal, we rely on contrastive loss that is widely used in self-supervised learning [5, 13] for pretraining. In particular, we adjust the global contrastive loss to a supervised pixel level loss, and construct a pixel-to-class prototype mapping, such that the pixel embeddings with the same label enjoy better intra-class compactness and inter-class separability, which we find is beneficial for semantic segmentation task. Considering that classes from different datasets may share similar embeddings, to better modeling inter-class relationship defined by the provided labels, we enrich the pixel level embeddings via cross dataset mixing and extend the pixel-to-class mapping, which can be treated as hard encoding using the provided annotations to sparse coding, which considers the relationship of similar classes. In this way, the pixel level embedding is endowed with a more smooth representation, which is beneficial for better transferability. Experiments conducted on several benchmarks demonstrate its superior performance.

In a nutshell, this paper makes the following contributions:

- We propose a novel pretraining setting that is able to effectively make use of the available annotations off-the-shelf by unifying multiple datasets without considering label integration. As far as we know, we are the first to unify multiple labeled datasets for pretraining, while not be bothered by the chaotic labels from diverse datasets.
- We propose a pixel-to-prototype mapping to effectively model intra-class compactness and inter-class separability. To better make use of cross dataset samples, we enrich the pixel embeddings via cross dataset mixing and extend the pixel-to-class hard coding to cross-class mapping via pixel-to-class sparse coding.
- MDP surpasses ImageNet pretraining by a large margin, with less than 10% samples comparing with models pretrained over ImageNet. Our findings validate that it is unnecessary for semantic segmentation to make use of classification as a pretext task, this may shed light on future research direction with respect to designing an appropriate pretrained model for semantic segmentation.

2 Related Work

Contrastive learning. Contrastive learning-based methods learn representations by contrasting positive pairs against negative pairs in a discriminative fashion. Recent works mainly benefits from instance discrimination [26], which regards each image and its augmentations as one separate class and others are negatives [13, 5, 8, 6, 15, 22, 24, 11]. Since using a large number of negatives is crucial for the success of contrastive loss-based representation learning, [26] uses a memory bank to store the pre-computed representations from which positive examples are retrieved given a query.

Based on it, [13] uses a momentum update mechanism to maintain a long queue of negative examples for contrastive learning.

Thanks to recent explorations in supervised contrastive learning [16] and pixel level contrastive learning [27], some recent works introduce contrast learning into semantic segmentation tasks [31, 20, 1, 25, 10] by pulling close the embedding of pixels with the same label and pushing apart the embedding of pixels with different labels. However, these methods do not explore the wide applicability of pixel level contrastive learning, and lack innovation in the pixel level loss design.

Multiple datasets training. For recognition tasks like object detection and semantic segmentation, training on naively combined datasets yields low accuracy and poor generalization [17] since different datasets have different class definitions and class granularity. Dataset unification, which involves merging different semantic concepts, is important for multi-dataset training. [18] manually builds a semantic concept hierarchy by combining labels from all four popular datasets and explicitly incorporates the hierarchy into network construction. [17] manually unifies the taxonomies of 7 semantic segmentation datasets and uses Amazon Mechanical Turk to resolve inconsistent annotations between datasets. However, these methods need heavily manual effort. [30] and [33] trains a universal detector by first training a single partitioned detector on multiple datasets with shared backbone dataset-specific outputs, and loss and then unifies the outputs of the partitioned detector in a common taxonomy. These methods still rely on partitioned learning on their respective datasets. Unlike these works, we do not unify their label space but make the pixel level features distinguishable by multiple datasets pretraining.

3 Method

In this section, we elaborate on our proposed multi-dataset pretraining strategy. The whole procedure is shown in Fig. 2. Given a set of samples with pixel level annotations, we aim at constructing pixel-to-class prototype mapping to model intra-class compactness and inter-class separability. The core modules consist of two parts, 1) pixel-to-prototype contrastive loss and 2) cross dataset learning, which would be explained in detail in the following sections.

3.1 Preliminaries

Contrastive learning targets at training an encoder to map positive pairs to similar representations while pushing away the negative samples in the embedding space. Given unlabeled training set $\mathbf{X} = \{x_1, x_2, \dots, x_n\}$. Instance-wise contrastive learning aims to learn an encoder E_q that maps the samples \mathbf{X} to embedding space $\mathbf{V} = \{v_1, v_2, \dots, v_n\}$ by optimizing a contrastive loss. Take the Noise Contrastive Estimator (NCE) [22] as an example, the contrastive loss is defined as:

$$\mathcal{L}_{nce}(x_i, x'_i) = -\log \frac{\exp(E_q(x_i) \cdot E_k(x'_i)/\tau)}{\exp(E_q(x_i) \cdot E_k(x'_i)/\tau) + \sum_{j=1}^K \exp(E_q(x_i) \cdot E_k(x'_j)/\tau)}, \quad (1)$$

where τ is the temperature parameter, and x'_i and x'_j denote the positive and negative samples of x_i , respectively. The encoder E_k can be shared [5, 3] or momentum update of the encoder E_q [13].

3.2 Pixel-to-pixel Contrastive Learning

Inspired by contrastive learning, we first present a simple baseline that directly extends the instance level contrastive learning to pixel level, guided by the provided pixel level annotations. In this setting, pixels with the same label are treated as positive pairs and pulled together, while those with different labels are regarded as negative pairs and pushed away. Note that since we constrain the positive samples within the same label, making it conveniently applicable for multiple datasets.

Specifically, given multiple labeled datasets $\mathcal{D} = \{\mathcal{D}_1, \mathcal{D}_2, \dots, \mathcal{D}_N\}$ along with label space $\mathcal{Y} = \{\mathcal{Y}_1, \mathcal{Y}_2, \dots, \mathcal{Y}_N\}$, we randomly select n samples $\{x_t\}_{t=1}^n$ from \mathcal{D} regardless of which domain each sample comes from. Denote \hat{x}_t and \bar{x}_t be two different augmented views of image x_t , with ground truth pixel level class label map $\hat{Y} = [\hat{y}_i \in \mathcal{Y}]$ and $\bar{Y} = [\bar{y}_i \in \mathcal{Y}]$, where i denotes pixel in the image. \hat{x}_t and \bar{x}_t are separately sent to feature extractor E_q and E_k to obtain d -dimensional per-pixel unit-normalized features $\hat{F} = [\hat{f}_i]$ and $\bar{F} = [\bar{f}_i]$, where E_k is a momentum update version of E_q . For

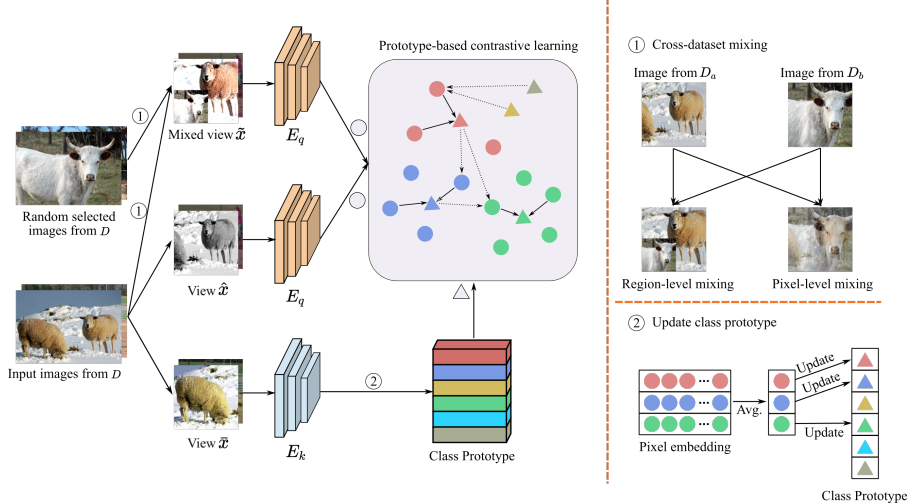


Figure 2: The overall pipeline of MDP. Given labeled image x randomly sampled from a collection of multiple datasets \mathcal{D} , we first obtain two different views \hat{x} and \bar{x} through data augmentation as well as a mixed view \tilde{x} through cross-dataset mixing with a sample that is also randomly selected from \mathcal{D} . Then we conduct class-to-prototype sparse coding to model intra-class compactness and inter-class separability, as well as considering cross-class similarity. The right part illustrates two components of MDP, *i.e.*, cross-dataset mixing and online class prototype update.

pixel i in \hat{F} , the pixel j in \bar{F} with the same class label is considered as positive sample of i , and the pixel level contrastive loss is computed by:

$$\mathcal{L}_{pixel} = -\frac{1}{\bar{N}_{y_i}} \sum_{j=1}^N \mathbb{1}[\hat{y}_i = \bar{y}_j] \log \left(\frac{\exp(\hat{f}_i \cdot \bar{f}_j / \tau)}{\sum_{k=1}^N \exp(\hat{f}_i \cdot \bar{f}_k / \tau)} \right), \quad (2)$$

where $N = \hat{N} = \bar{N}$ denotes the total number of pixels in each view and \bar{N}_y denotes the number of pixels with class y in \bar{x}_t . The loss is averaged over all pixels on the first view. Similarly, the contrastive loss for pixel j on the second view is also computed and averaged.

The pixel level contrastive loss enables multi-dataset training and does not need to consider the label mapping, since the calculation of pixel level contrastive loss is independent for each image. However, such a pixel-to-pixel optimization strategy is sensitive to noisy annotations and more importantly, it does not consider the relationship across datasets, which limits its representation ability. In the following, we extend this baseline to support modeling relationships among different images and different classes for better pretraining.

3.3 Pixel-to-prototype Contrastive Learning

Considering that the pixel level representation is less meaningful than the instance-level one, and may suffer great difference even for embeddings with the same label, such representation uncertainty makes the pixel-to-pixel optimization goal fluctuate and hard for convergence. To solve this issue, we adjust the pixel-to-pixel contrastive learning with more robust pixel-to-class mapping. The motivation is that class-level representation is more stable and memory-efficient comparing with recording pixel level embeddings. In particular, we merge the label spaces of the collection of all datasets \mathcal{D} and obtain class set $\mathcal{Y} = \mathcal{Y}_1 \cup \mathcal{Y}_2 \cup \dots \cup \mathcal{Y}_n$. We maintain a prototype for each class $y_i \in \mathcal{Y}$ in the memory bank. Then we learn the embeddings of all the pixels in each input image x by pulling them close to the same class prototype and pushing them apart to different class prototypes.

Class prototype. A key component for pixel-to-prototype mapping is to maintain the prototype for each class. Considering that the labeling granularity is at pixel level, which is huge and memory-consuming, we propose an efficient prototype maintenance strategy to dynamically update the class

embeddings. Specifically, suppose we have a total of N training images and $|\mathcal{Y}|$ semantic classes. Let P_y be the class prototype of class y , we first calculate the embedding of class y for n -th images, represented by p_{ym} , by average pooling of all the embeddings of pixels labeled as y in the n -th image. Then, P_y is obtained by averaging all embeddings among N images that contain class y :

$$P_y = \frac{\sum_{i=1}^N m_{yi} p_{yi}}{\sum_{i=1}^N m_{yi}}, \quad (3)$$

where $m_{yi} \in [0, 1]$ is a binary mask indicating whether the i th-image contains pixels with class y . In practice, in order to realize the dynamic update of P_y , we store the embedding sum of class c and the number of images that contain pixels with class c for each batch b . Some works [25, 10] propose region embedding strategy, which simply stores the image embedding set $P'_y = \{p_{y1}, p_{y2}, \dots, p_{yN}\}$ for class y in the memory bank. We argue that our two step average strategy for prototype calculation can bring three advantages comparing with region embedding:

- **Reducing the storage requirements.** The memory bank of region embedding is built with size $|\mathcal{Y}| \times N_b \times Dim$, where Dim indicates the dimension of pixel embedding and N_b indicates the number of image embeddings saved in the memory bank. Its storage consumption will become large as the growth of N_b and $|\mathcal{Y}|$. While using the class prototype, we can reduce the size to $|\mathcal{Y}| \times B \times Dim$ while maintaining the dynamic update of P_y , where $B = N_b/b_s$ is the total number of batches and b_s means the batch size.
- **Alleviating the class imbalance problem especially when using multiple datasets.** Our method obtains one prototype for each class y , regardless of the number of images containing y . This ensures the contribution of small datasets and classes with rare data be not ignored.
- **Obtaining more robust class embeddings.** The prototypes we provide for each class are not susceptible to dirty data and are representative enough since it is obtained by considering the embeddings of all pixels with the same class.

Loss function. In prototype-based contrastive learning, we first update the prototype in the memory bank using \bar{F} according to (3). Then, for pixel i with class j in \hat{x} , we maximize the agreement between its embedding \hat{f}_i and the prototype of class j . Additionally, we require a push-force to avoid collapse in the embedding space. This can be achieved by pushing \hat{f}_i and other class prototypes apart. The prototype-based contrastive loss for pixel i is computed by:

$$\mathcal{L}_{class} = -\mathbb{1}[\hat{y}_i = j] \log \left(\frac{\exp(\hat{f}_i \cdot P_j / \tau)}{\sum_{k=1}^{|\mathcal{L}|} \exp(\hat{f}_i \cdot P_k / \tau)} \right) \quad (4)$$

The final loss is also computed for pixels from two different views and then averaged. Pixel embeddings in current image are not only influenced by the same class pixels in other images, but also interactive with the classes which do not occur in current image. Prototype-based contrastive learning makes the learning of embedding not confined to a single image, which greatly improves the embedding quality compared to pixel-to-pixel contrastive learning.

3.4 Cross Dataset Learning

The pixel-to-prototype mapping can be treated as hard coding for each pixel, and the codes are simply generated by averaging operations using the provided pixel level labels. While in real applications, classes from different datasets may share similar embeddings. In order to better model the inter-class relationship defined by the provided labels, we propose two cross dataset interaction operations. First, we enrich the pixel level embeddings via cross dataset mixing. And second, we extend the pixel-to-class hard mapping to more general soft mapping. In this way, the pixel level embedding is endowed with a more smooth representation, which is beneficial for better transferability.

Cross-image pixel representation. We adopt two different levels of data mixing methods, *i.e.*, region-level mixing and pixel-level mixing, to interact representation across different datasets. We argue that data mixing is intrinsically suitable for pixel level tasks, though it is first proposed for improving classification on ImageNet [23]. These two mixing methods alleviate the problem of input inconsistency and class inconsistency from different perspectives, and they are complementary.

Region-level mixing Given two labeled images $\{x_i, y_i\}, \{x_j, y_j\}$ from the collection of all datasets \mathcal{D} , we conduct cross-dataset cutmix [28] operation by:

$$\begin{aligned}\tilde{x} &= M \odot x_i + (1 - M) \odot x_j \\ \tilde{y} &= M \odot y_i + (1 - M) \odot y_j\end{aligned}\tag{5}$$

where M denotes a binary mask indicating where to dropout and fill in from two images, and \odot is element-wise multiplication. The mixed image can interact with the prototype in the same way as before. Region-level mixing enables the model to see different regions of different datasets at the same time, which can reduce the gap between different datasets. At the same time, region-level mixing destroys the regional continuity of the original image, making the model pay more attention to pixel level details and also increase the diversity of features.

Pixel-level mixing Also, given two random samples $\{x_i, y_i\}, \{x_j, y_j\}$, we can conduct cross-dataset pixel-level mixing using mixup [29] operation:

$$\begin{aligned}\tilde{x} &= \lambda x_i + (1 - \lambda)x_j \\ \tilde{y} &= \{\lambda, y_i, y_j\}\end{aligned}\tag{6}$$

Where $\lambda \in [0, 1]$. It should be noted that the class label should be an integer, so we do not mix the label but storing the set $\{\lambda, y_i, y_j\}$ in \tilde{y} . the final loss $\mathcal{L}(\tilde{x}, \tilde{y}, P)$ can be obtained by considering the contribution of the two groundtruth labels, y_i and y_j , using the class prototype P and weight λ :

$$\mathcal{L}(\tilde{x}, \tilde{y}, P) = \lambda \mathcal{L}(\tilde{x}, y_i, P) + (1 - \lambda) \mathcal{L}(\tilde{x}, y_j, P).\tag{7}$$

Pixel-level mixing can integrate the image information from different datasets in a more fine-grained way. In addition, pixels will contain contents from different classes, which makes up for inconsistencies across datasets at both image and class levels.

Cross-class sparse coding. We explicitly model the inter-class similarity via extending the pixel-to-prototype hard coding to soft coding, *i.e.*, in addition to pushing the embedding of pixel i close to its corresponding ground-truth class prototype, we also push its embedding close to its top- K similar class prototypes:

$$\mathcal{L}_{sc} = -\alpha * \mathbb{1}[y_i = j] \log \left(\frac{\exp(\hat{f}_i \cdot P_j / \tau)}{\sum_{k=1}^{|L|} \exp(\hat{f}_i \cdot P_k / \tau)} \right) - (1 - \alpha) \frac{1}{K} \sum \mathbb{1}[t \in T] \log \left(\frac{\exp(\hat{f}_i \cdot P_t / \tau)}{\sum_{k=1}^{|L|} \exp(\hat{f}_i \cdot P_k / \tau)} \right), \tag{8}$$

where T denotes the set of top- K similar class prototypes of i . α is simply set to 0.5 and K is 5 by default. Our method provides an elegant way to utilize the class similarity of different datasets to help improve the diversity of pixel features.

4 Experiments

In this section, we evaluate MDP on several widely used benchmarks, as well as a detailed ablation study to reveal how each module affects the final performance.

4.1 Experimental Setups

Datasets. Our experiments are conducted on four datasets, namely:

- **Cityscapes** [7] has 5,000 finely annotated urban scene images, with 2,975/500/1,524 for train/val/test, respectively. The segmentation performance is reported on 19 challenging categories, such as person, sky, car, and building *etc.*
- **Pascal VOC 2012** [9] consists of 10,582 training (including the annotations provided by [12]), 1,449 validation, and 456 test images with pixel level annotations for 20 foreground object classes and one background class.
- **ADE20K** [32] contains around 25K images spanning 150 semantic categories, of which 20K for training, 2K for validation, and another 3K for testing.
- **COCO-Stuff** [2] is a large scale dataset, which includes 164K images from COCO 2017 [19]. Among them, 118k images are used for training and 5k images are used for validation. It provides rich annotations for 80 object classes and 91 stuff classes.

Table 1: Overall results evaluated on three different datasets: Pascal VOC, ADE20K and Cityscapes, using different amount of datasets for pretraining.

Method	Pretrained Dataset				Epoch	mIoU		
	ImageNet	VOC	ADE20K	COCO		VOC	ADE20K	Cityscapes
Scratch					-	44.78	28.67	54.27
MoCo-v2	✓				800	71.59	38.29	77.52
Supervised	✓				-	75.63	39.36	77.60
MDP		✓	✓		100	73.32	40.17	77.75
MDP		✓	✓		200	74.30	40.83	78.59
MDP		✓	✓	✓	200	77.79	42.69	80.64

Evaluation. We choose the training split of Pascal VOC and ADE20K for pretraining since they are comparable at scale, and evaluate the performance on the two datasets to validate how pretraining using other datasets boosts the performance. We also transfer the pretrained model to Cityscapes, where the model does not see during the pretraining stage to validate its generalization ability. Finally, we add COCO-Stuff for pretraining to validate how large scale dataset helps for pretraining. Following the standard setting, we choose mean Intersection-over-Union (mIoU) for performance evaluation.

Implementation details. We choose DeepLab-v3 [4] based on a standard ResNet-50 as backbone [14]. Following the settings in MoCo-v2 [6], we employ an asynchronously updated key encoder and adds a 4-layer projection head after the ASPP layer of the DeepLab-v3 model, which finally results in a 256-d embedding vector for each pixel. The model is pretrained using an SGD optimizer with momentum 0.9 and weight decay $4e-5$. The batch size and the initial learning rate are set to 32 and 0.2 respectively, over 2 NVIDIA Tesla V100 GPUs. The learning rate is decayed to 0 by cosine scheduler [21]. The input size is set to 224×224 for efficiency. We use the same set of augmentations as in MoCo-v2. The temperature parameter τ of contrastive loss is set to 0.07, and the size of the memory bank is approximately equal to the total number of batches.

During the downstream fine-tuning stage, we follow the basic configure of MMsegmentation¹ except substituting the backbone with a standard ResNet-50 and removing the auxiliary head. Other settings follow the default configurations as in MMsegmentation. For Pascal VOC, we fine-tune the pretrained model for $40k$ iterations using 513×513 input size, while for ADE20K, the iterations are set to $80k$ with 512×512 input size, and for Cityscapes, the iterations are set as $40k$ with 512×1024 input size. *Note that our implementation aims to show the effectiveness of multi-dataset pretraining and use some basic settings and structure for evaluation.* While there are several tricks to further improve the performance, such as larger resolution for pretraining and more advanced structure with auxiliary head, this is out of the scope of this paper.

4.2 Results

In this section, we report the overall results when fine-tuning on three datasets: Pascal VOC, ADE20K, and Cityscapes. As shown in Table 1, for completeness, we also list the results of using other pretrained models, which includes: a) train from scratch with random initialization; b) self-supervised model based on MoCo-v2 using ImageNet as pretraining data; c) fully supervised model on ImageNet. We report the results for pretraining over both 100 and 200 epochs. From this table we find that:

Comparing with other pretrained models. All pretraining models surpass train from scratch by a large margin, and MDP beats both supervised and self-supervised ImageNet pretrained models. Specifically, when using only Pascal VOC and ADE20K (around 30K images) for pretraining, we achieve 74.30% and 40.83% accuracies on Pascal VOC and ADE20K, respectively. The performance can be further improved by adding a large scale COCO Stuff dataset, which surpasses the fully supervised model by a noticeable margin, that is 2.16% performance gain (75.63% \rightarrow 77.79%) on Pascal VOC, 3.33% gain (39.36% \rightarrow 42.69%) on ADE20K. It should be noted that compared to ImageNet pretraining, MDP only uses less than 10% samples for pretraining, which is more efficient.

¹<https://github.com/open-mmlab/msegmentation>

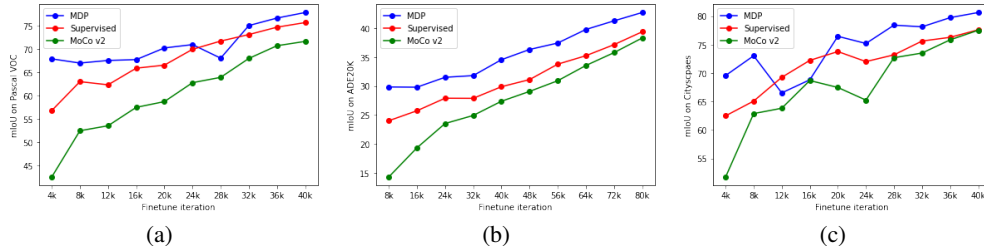


Figure 3: Comparisons of MDP, MoCo-V2, and supervised ImageNet pretraining on a) Pascal VOC, b) ADE20k and c) Cityscapes at different fine-tuning iterations. MDP consistently outperforms the other two models throughout the training procedure.

Table 2: Ablation studies on hyper-parameters and the type of memory bank.

Method	Memory Bank Type	Memory Bank Size	Temperature τ	mIoU
pixel-to-pixel			0.07	68.05
MDP	Region	4096	0.07	68.69
MDP	Class	4096	0.07	69.72
MDP	Class	1024	0.07	69.61
MDP	Class	4096	0.07	69.72
MDP	Class	10560	0.07	69.8
MDP	Class	4096	0.07	69.72
MDP	Class	4096	0.3	69.01
MDP	Class	4096	0.5	68.65

Transfer ability. We also evaluate the performance on Cityscapes, where the model does not see any images over this dataset during pretraining, and the results are surprisingly promising. When only using Pascal VOC and AED20K for pretraining, we achieve 78.59% accuracy, which is already 1% better than the fully supervised model on ImageNet, and the performance can be further boosted to 80.64% when adding COCO-Stuff for pretraining. The results indicate that MDP also enjoys better transferability.

4.3 Ablation Study

In this section, we conduct extensive ablation studies to better understand how each component affects the performance. **Unless specified, all models are pretrained over Pascal VOC for 100 epochs and evaluated on Pascal VOC for efficiency.**

Hyperparameter analysis. Table 2 studies the influence of the temperature τ and the memory bank size N_b . Note that the actual size of the class prototype in our implementation is N_b/b_s . We conclude that the proposed algorithm is relatively robust to memory bank size N_b when sufficient samples are stored in the memory bank. We also find that the temperature $\tau = 0.07$ brings better performance under supervised pixel level contrastive learning setting, which is different from self-supervised learning where τ is usually larger ($\tau = 0.2$ in MoCo-v2). The reason is that τ controls the strength for contrastive learning, with smaller τ indicating stronger penalizing for compactness and separability. It makes sense that pixel level contrastive learning gets better results for small τ since it is guided by ground truth labels.

Effects of class prototype. Table 2 reveals the effectiveness of class prototype. Our method surpasses pixel-to-pixel contrastive learning baseline (r.f. Sec. 3.2) by 1.67%. Compared with the region-based prototype (r.f. Sec. 3.3) which stores the embedding of each image by class, our method obtains 1.03% performance gain (68.69% to 69.72%). This is mainly due to that our method can obtain more representative embedding and has the ability to resist the class imbalance problem.

Table 3: Comparisons of different cross-dataset mixing strategy.

Method	Pretrained Dataset		Augmentation Type		mIoU
	VOC	ADE20K	Region-level	Pixel-level	
MDP	✓				69.72
	✓		✓		70.92
	✓			✓	68.40
MDP	✓	✓			71.98
	✓	✓	✓		72.66
	✓	✓		✓	73.00
	✓	✓	✓	✓	73.32

Table 4: Results of utilizing cross-class sparse coding.

Method	Pretrained Dataset		Sparse coding	mIoU	
	VOC	ADE20K		VOC	Cityscapes
MDP	✓	✓		71.98	75.37
MDP	✓	✓	✓	71.84	76.53

Effects of cross-dataset mixing. Table 3 inspects the influence of cross-dataset mixing. It can be seen that when both pretraining and evaluation are performed on Pascal VOC, only region-level mixing can bring gains. We think this is because pixel-level mixing changes the distribution of labels, which is not beneficial when using the same, single dataset for pretraining. However, when extended to multiple datasets, both mixing methods bring significant performance improvements (0.69% gains for region-level mixing and 1.02% gains for pixel-level mixing), and combining them brings another improvement (73.32%).

Effects of cross-class sparse coding. We also diagnose the effectiveness of cross-class sparse coding. As shown in Table 4, cross-class sparse coding brings 1.16% performance improvement on Cityscapes, from 75.37% to 76.53% but achieves no performance gain on Pascal VOC dataset (71.84% compared to 71.98%). We think this is because both pretraining and fine-tuning make use of Pascal VOC data. In this case, it may be more effective to directly separate the label space of Pascal VOC from the label space of other datasets. While sparse coding is suitable for better transferability.

Does MDP obtain more discriminative features? Fig. 3 compares the evaluation results of MDP and ImageNet pretraining at different fine-tuning iterations over three datasets. It can be seen that the performance of MDP is substantially higher than ImageNet pretrained model. It should be noted that at the beginning of fine-tuning, MDP has achieved far better performance, even for Cityscapes that the model does not see during the pretraining stage, which proves that MDP can obtain more discriminative features due to pixel level learning. MoCo-v2 suffers the worst initial performance, which also indicates that the instance-level contrast learning cannot handle pixel level semantic segmentation tasks well.

5 Conclusion

This paper proposed a multi-dataset pretraining framework for semantic segmentation, which can efficiently make use of the off-the-shelf annotations to construct a better and more general pretrained model. The main contributions are two folds. First, we propose a pixel-to-class prototype contrastive loss to effectively model intra-class compactness and inter-class separability of multiple datasets regardless of their taxonomy labels. Second, we extend the pixel level embeddings via cross dataset mixing and pixel-to-class sparse coding for better transferability. Our method consistently outperforms the pretrained models over ImageNet on several widely used benchmarks, while using much fewer samples for pretraining. Although MDP only makes use of fully labeled data for pretraining currently, our method is able to conveniently extended to the semi-supervised scenario, which remains to be explored in the future work.

References

- [1] Inigo Alonso, Alberto Sabater, David Ferstl, Luis Montesano, and Ana C. Murillo. Semi-supervised semantic segmentation with pixel-level contrastive learning from a class-wise memory bank. *arXiv preprint arXiv:2104.13415*, 2021.
- [2] Holger Caesar, Jasper Uijlings, and Vittorio Ferrari. Coco-stuff: Thing and stuff classes in context. In *IEEE/CVF Conference on Computer Vision and Pattern Recognition (CVPR)*, 2018.
- [3] Mathilde Caron, Ishan Misra, Julien Mairal, Priya Goyal, Piotr Bojanowski, and Armand Joulin. Unsupervised learning of visual features by contrasting cluster assignments. *arXiv preprint arXiv:2006.09882*, 2020.
- [4] Liang-Chieh Chen, Yukun Zhu, George Papandreou, Florian Schroff, and Hartwig Adam. Encoder-decoder with atrous separable convolution for semantic image segmentation. In *Proceedings of the European Conference on Computer Vision (ECCV)*, pages 833–851, 2018.
- [5] Ting Chen, Simon Kornblith, Mohammad Norouzi, and Geoffrey Hinton. A simple framework for contrastive learning of visual representations. *arXiv preprint arXiv:2002.05709*, 2020.
- [6] Xinlei Chen, Haoqi Fan, Ross Girshick, and Kaiming He. Improved baselines with momentum contrastive learning. *arXiv preprint arXiv:2003.04297*, 2020.
- [7] Marius Cordts, Mohamed Omran, Sebastian Ramos, Timo Rehfeld, Markus Enzweiler, Rodrigo Benenson, Uwe Franke, Stefan Roth, and Bernt Schiele. The cityscapes dataset for semantic urban scene understanding. In *IEEE/CVF Conference on Computer Vision and Pattern Recognition (CVPR)*, pages 3213–3223, 2016.
- [8] Alexey Dosovitskiy, Philipp Fischer, Jost Tobias Springenberg, Martin Riedmiller, and Thomas Brox. Discriminative unsupervised feature learning with exemplar convolutional neural networks. *IEEE Transactions on Pattern Analysis and Machine Intelligence*, 38(9):1734–1747, 2015.
- [9] Mark Everingham, S. M. Ali Eslami, Luc Van Gool, Christopher K. I. Williams, John M. Winn, and Andrew Zisserman. The pascal visual object classes challenge: A retrospective. *International Journal of Computer Vision (IJCV)*, 111(1):98–136, 2015.
- [10] Wouter Van Gansbeke, Simon Vandenhende, Stamatios Georgoulis, and Luc Van Gool. Unsupervised semantic segmentation by contrasting object mask proposals. *arXiv preprint arXiv:2102.06191*, 2021.
- [11] Jean-Bastien Grill, Florian Strub, Florent Altché, Corentin Tallec, Pierre H Richemond, Elena Buchatskaya, Carl Doersch, Bernardo Avila Pires, Zhaohan Daniel Guo, Mohammad Gheshlaghi Azar, et al. Bootstrap your own latent: A new approach to self-supervised learning. *arXiv preprint arXiv:2006.07733*, 2020.
- [12] Bharath Hariharan, Pablo Arbelaez, Lubomir D. Bourdev, Subhransu Maji, and Jitendra Malik. Semantic contours from inverse detectors. In *Proceedings of the IEEE Conference on Computer Vision and Pattern Recognition (CVPR)*, pages 991–998, 2011.
- [13] Kaiming He, Haoqi Fan, Yuxin Wu, Saining Xie, and Ross Girshick. Momentum contrast for unsupervised visual representation learning. In *Proceedings of the IEEE/CVF Conference on Computer Vision and Pattern Recognition (CVPR)*, pages 9729–9738, 2020.
- [14] Kaiming He, Xiangyu Zhang, Shaoqing Ren, and Jian Sun. Deep residual learning for image recognition. In *Proceedings of the IEEE conference on computer vision and pattern recognition (CVPR)*, pages 770–778, 2016.
- [15] R Devon Hjelm, Alex Fedorov, Samuel Lavoie-Marchildon, Karan Grewal, Phil Bachman, Adam Trischler, and Yoshua Bengio. Learning deep representations by mutual information estimation and maximization. *arXiv preprint arXiv:1808.06670*, 2018.
- [16] Prannay Khosla, Piotr Teterwak, Chen Wang, Aaron Sarna, Yonglong Tian, Phillip Isola, Aaron Maschinot, Ce Liu, and Dilip Krishnan. Supervised contrastive learning. *arXiv preprint arXiv:2004.11362*, 2020.
- [17] John Lambert, Zhuang Liu, Ozan Sener, James Hays, and Vladlen Koltun. Mseg: A composite dataset for multi-domain semantic segmentation. In *IEEE/CVF Conference on Computer Vision and Pattern Recognition (CVPR)*, pages 2876–2885, 2020.

- [18] Xiaodan Liang, Eric Xing, and Hongfei Zhou. Dynamic-structured semantic propagation network. In *IEEE/CVF Conference on Computer Vision and Pattern Recognition (CVPR)*, pages 752–761, 2018.
- [19] Tsung-Yi Lin, Michael Maire, Serge Belongie, James Hays, Pietro Perona, Deva Ramanan, Piotr Dollár, and C Lawrence Zitnick. Microsoft coco: Common objects in context. In *Proceedings of the European Conference on Computer Vision (ECCV)*, pages 1209–1218, 2014.
- [20] Shikun Liu, Shuaifeng Zhi, Edward Johns, and Andrew J. Davison. Bootstrapping semantic segmentation with regional contrast. *arXiv preprint arXiv:2104.04465*, 2021.
- [21] Ilya Loshchilov and Frank Hutter. Sgdr: Stochastic gradient descent with warm restarts. *arXiv preprint arXiv:1608.03983*, 2016.
- [22] Aaron van den Oord, Yazhe Li, and Oriol Vinyals. Representation learning with contrastive predictive coding. *arXiv preprint arXiv:1807.03748*, 2018.
- [23] Olga Russakovsky, Jia Deng, Hao Su, Jonathan Krause, Sanjeev Satheesh, Sean Ma, Zhiheng Huang, Andrej Karpathy, Aditya Khosla, Michael Bernstein, et al. Imagenet large scale visual recognition challenge. *International journal of computer vision (IJCV)*, 115(3):211–252, 2015.
- [24] Yonglong Tian, Dilip Krishnan, and Phillip Isola. Contrastive multiview coding. *arXiv preprint arXiv:1906.05849*, 2019.
- [25] Wenguan Wang, Tianfei Zhou, Fisher Yu, Jifeng Dai, Ender Konukoglu, and Luc Van Gool. Exploring cross-image pixel contrast for semantic segmentation. *arXiv preprint arXiv:2101.11939*, 2021.
- [26] Zhirong Wu, Yuanjun Xiong, Stella X Yu, and Dahua Lin. Unsupervised feature learning via non-parametric instance discrimination. In *Proceedings of the IEEE Conference on Computer Vision and Pattern Recognition (ICCV)*, pages 3733–3742, 2018.
- [27] Zhenda Xie, Yutong Lin, Zheng Zhang, Yue Cao, Stephen Lin, and Han Hu. Propagate yourself: Exploring pixel-level consistency for unsupervised visual representation learning. *arXiv preprint arXiv:2011.10043*, 2020.
- [28] Sangdoon Yun, Dongyoon Han, Seong Joon Oh, Sanghyuk Chun, Junsuk Choe, and Youngjoon Yoo. Cutmix: Regularization strategy to train strong classifiers with localizable features. In *Proceedings of the IEEE International Conference on Computer Vision (CVPR)*, pages 6023–6032, 2019.
- [29] Hongyi Zhang, Moustapha Cisse, Yann N Dauphin, and David Lopez-Paz. mixup: Beyond empirical risk minimization. *arXiv preprint arXiv:1710.09412*, 2017.
- [30] Xiangyun Zhao, Samuel Schuster, Gaurav Sharma, Yi-Hsuan Tsai, Manmohan Chandraker, and Ying Wu. Object detection with a unified label space from multiple datasets. In *Proceedings of the European Conference on Computer Vision (ECCV)*, pages 178–193, 2020.
- [31] Xiangyun Zhao, Raviteja Vemulapalli, Philip Andrew Mansfield, Boqing Gong, Bradley Green, Lior Shapira, and Ying Wu. Contrastive learning for label-efficient semantic segmentation. *arXiv preprint arXiv:2012.06985*, 2020.
- [32] Bolei Zhou, Hang Zhao, Xavier Puig, Tete Xiao, Sanja Fidler, Adela Barriuso, and Antonio Torralba. Semantic understanding of scenes through the ade20k dataset. *International Journal on Computer Vision (IJCV)*, 127:302–321, 2019.
- [33] Xingyi Zhou, Vladlen Koltun, and Philipp Krähenbühl. Simple multi-dataset detection. *arXiv preprint arXiv:2102.13086*, 2021.